Volume 21, No 3 | International Journal of Radiation Research, July 2023

Monte Carlo calculations of critical organ doses in radioembolization therapy of primary liver tumors via ^{90}Y microspheres

O.M. Yildirim[1], A. Bingolbali[1,2*], A. Bozkurt[3], C. Cafaro[4], M.O. Demirkol[5]

[1]Department of Bioengineering, Yildiz Technical University, 34220 Istanbul, Turkey
[2]Department of Physics, University at Albany-SUNY, 12222 Albany, NY, USA
[3]Department of Biomedical Engineering, Akdeniz University, 07058 Antalya, Turkey
[4]Department of Mathematics & Physics, SUNY Polytechnic Institute, 12222 Albany, NY, USA
[5]Department of Nuclear Medicine & Molecular Imaging, Koç University, 34450 Istanbul, Turkey

► ***Original article***

Corresponding author:
Ayhan Bingolbali, Ph.D.,
E-mail: *ab1353@gmail.com*

Received: May 2022
Final revised: September 2022
Accepted: September 2022

Int. J. Radiat. Res., July 2023; 21(3): 353-360

DOI: 10.52547/ijrr.21.3.1

Keywords: *Radioembolization, ^{90}Y, critical organ doses, MIRD, Monte Carlo simulations.*

ABSTRACT

Background: Dosimetry calculations in radioembolization therapy are known to include some uncertainties due to working assumptions. First, the microspheres used in the procedure are homogeneously distributed within the tumor volume. Second, Medical Internal Radiation Dosimetry (MIRD) method of dose calculation involves a mono-compartmental model only. To minimize the impact of these uncertainties, this study proposes Monte Carlo (MC) simulations as an alternative to MIRD method to verify the absorbed doses in the volumes of interest (tumor and its surroundings). ***Material and Methods***: Lung, liver, and tumor volumes of 30 radioembolization patients were defined in a mathematical whole-body phantom and MC simulations were performed using Monte Carlo N-Particle code. Absorbed doses were calculated for these tissues both in addition to stomach wall, pancreas, spleen, and kidneys which are close to the tumor volume being treated with microspheres of radioembolization therapy containing the beta-emitting ^{90}Y radioisotope. ***Results***: The doses absorbed by tumor, lung, and liver volumes of each patient were calculated by both MIRD methodology and MC simulations. The differences between the two methods were evaluated for normal lung tissue and tumor tissues in the liver where maximum differences were observed for tumor tissues (16.18%) and lungs (11.69%). Furthermore, it was observed through MC simulations; the organs that are close to the liver being treated were also exposed to the radiation for which absorbed doses could not be calculated by MIRD method. ***Conclusion***: MC simulations may offer significant advantages for dose verification in radioembolization therapy.

INTRODUCTION

Radioembolization is a form of brachytherapy usually prescribed for primary and metastatic liver tumors when resistance to chemotherapy may develop or when portal vein occlusion exists [1]. Also known by various names such as intra-arterial radionuclide therapy (IRT), selective internal radionuclide therapy (SIRT), or trans-arterial radioembolization (TARE), this method is preferred for liver tumors that cannot be surgically resected and is applied by administering microspheres marked with ^{90}Y (Yttrium-90) radioactive isotope directly into the tumor site from the right or left hepatic artery, or a selected hepatic artery under the guidance of a catheter [2]. Beta particles emitted by the ^{90}Y radioisotope deliver a radiation dose to destroy the tumor and for some SIRT applications, embolization is tumoricidal in addition to irradiation [3].

^{90}Y radioisotope has a half-life of 64.2 hours and remains in the liver after decaying to stable Zirconium-90 (^{90}Zr). It is a beta emitter with maximum beta energy of 2.461 MeV, and average beta energy of 0.94 MeV [4]. The penetration of these beta energies in tissue can extend to 11 mm with the average range being 2.5 mm. Thus, most of the energy of ^{90}Y beta energies accumulates in the first few millimeters and concentrates at the location of the therapeutic microspheres [5]. In addition to beta energies, there is also a detectable peak of 511 keV photons due to internal pair production [6] which exceeds the continuous spectrum of bremsstrahlung photons which can be utilized by a gamma camera for image acquisition [7, 8].

Internal dosimetry plays an important role in nuclear medicine treatments [9]. Dosimetry calculations are available according to the type of microsphere used in radioembolization therapy. However, the dosimetry calculations create

[DOI: 10.61186/ijrr.21.3.353]

uncertainty due to some reasons, such as considering only one compartment and ignoring gamma penetration. To overcome these limitations, some researchers set up MC simulations tools and processed patient information into the program [10].

In the current work, we carried out a retrospective study on clinical cases SIRT of Hepatocellular Carcinoma (HCC) from primary liver tumors. For thirty cases (i.e., 30 patients) we set up MC internal dosimetry procedure of the Monte Carlo N-Particle (MCNP) package to estimate the absorbed dose distribution in liver's tumor and environing organs, especially on the lung due to pulmonary shunt.

Thus, this study aimed to calculate radiation doses that were calculated more accurately for organs of a patient to perform more sensitive therapy planning by using patient-specific information in calculations. For this purpose, an anthropomorphic mathematical body model developed specifically for MCNP was modified, for each patient to include the corresponding liver, tumor, and lung volumes. Monte Carlo method provided absorbed doses for the tumor and adjacent tissues of each radioembolization patient. Dosimetry calculations were also made for each patient with the MIRD method. In this manner, we attempted to improve the accuracy of Y-90 SIRT organ dose calculations of the mono-compartmental MIRD method by adopting a hybrid method that included a mathematical phantom, certain anatomical features of a patient and a MC radiation transport software.

MATERIAL AND METHODS

General characteristics of patients

The study was carried out on 30 patients. The median age of the patients in the study was 64. Twenty two patients (73%) were male and 8 were female (27%). The inclusion criteria of the patients in the study is given in table 1. Moreover, table 2 shows demographic characteristics of the patienst, such as; age, sex, body mass index, diagnosis methods for radioembolization patients, and mean baseline laboratory values. This study and its protocol were approved by the Ethics Committee of Koc University, Faculty of Medicine Clinical Research (Date: 30.10.2019/ No: 2019. 098.IRB1.010).

Dose calculations

If a patient is suitable for this therapy, radioembolization is performed by ^{90}Y radioisotope incorporated into the glass or resin microspheres. The decision on which type of microsphere to be used varies from clinic to clinic and heavily depends on the amount of activity to be applied. The patients included in this study were all administered by glass microspheres.

In clinical practice, radioembolization dosimetry is usually done using different dosimetry equations depending on the type of microsphere involved. For glass microspheres, for example, the mono-compartmental MIRD method can be preferred [11]. The meaning of 'compartment' word here refers to specific areas (for example, organs, tumors, normal tissue) irradiated by the microspheres and is mathematically treated as a separate unit by the dosimetry model. The mono-compartmental MIRD method, on the other hand, treats both tumor and non-tumor tissues as a single unit and does not differentiate between them [1, 11]. It only considers the total perfused liver volume and does not divide the liver tissue into separate volumes. This simplification, however, makes the absorbed dose calculations less precise.

Table 1. Inclusion criteria to Yttrium-90 (^{90}Y) microsphere radioembolization.

Inclusion criteria to ^{90}Y radioembolization
HCC Diagnosis
Albumin > 3 g/dL
Total bilirubin < 2 mg/dL
Thrombocyte > 50 K/uL
Haemoglobin > 9 g/dL
Tumor Volume < 50%
ECOG <3
AST and ALT < 5 × institutional ULN
INR < ×1.5
Portal vein thrombosis

HCC, Hepatocellular carcinoma; ECOG, Eastern Cooperative Oncology Group; ALT, alanine aminotransferase; AST, aspartate aminotransferase; INR, International Normalized Ratio ; ULN, upper limit of normal.

Table 2. Baseline characteristics.

Demographics	**Statistics***
Age(years)	
Median (Range)	63.5 (51-82)
<55 , *n (%)*	6 (20)
55-64 , *n (%)*	10 (33)
65+ , *n (%)*	14 (47)
Sex, *n (%)*	
Female	8 (27)
Male	22 (73)
BMI (kg/m^2), *n (%)*	
<25	8 (27)
25-29	17 (57)
30-34	4 (4)
35+	1 (3)
Method of diagnosis, *n (%)*	
Imaging	15 (50)
α-Fetoprotein level	15 (50)
Mean baseline laboratory values	
Bilirubin, total (mg/dL)	0.67
Serum albümin (g/dL)	4.06
ALT (U/L)	34.9
AST (U/L)	45.2
GGT (U/L)	238.9
INR	1.04
Hemoglobin (g/dL)	12
AFP (ng/mL)	2226.5
Trombosit (K/uL)	220

BMI, Body Mass Index; ALT, alanine aminotransferase; AST, aspartate aminotransferase; INR, International Normalized Ratio GGT, gamma glutamyl transferase; AFP, alpha fetoprotein. *N=30

[DOI: 10.61186/ijrr.21.3.353]

Absorbed dose calculations in liver and lung volumes (including shunt ratios) as well as tumor tissue by converting the activity [Bq] to the absorbed dose [Gy] as outlined in equation (1) [12]. For example, the MIRD formulation presented in this equation assumes that the dose delivered to the liver tissue results from the radioactivity administered to the patient and is localized within the perfused liver volume [1, 13].

$$D\,[Gy] = 50\left[\frac{J}{GBq}\right]\left(\frac{A_{total}[GBq]}{m_{liver}[kg]}\right) \quad (1)$$

Where; D[Gy] represents the dose value indicated for the liver volume, A[GBq] represents ^{90}Y activity applied to perfused liver, m_{liver}[kg] represents perfused liver mass.

If a fraction of the radionuclide activity is shunted to the lungs, it causes extrahepatic accumulation and contributes to the absorbed dose in the liver. If there is any pulmonary shunt, the total activity is divided between the liver and lung volumes as seen in equation (2) from which the dose delivered to the lungs can be calculated [1].

$$D_{lung}\,[Gy] = 50\left[\frac{J}{GBq}\right]\left(\frac{A_{total}[GBq]}{m_{lung}[kg]}\right)(LSF) \quad (2)$$

In Eq. (2), D_{lung} refers to the absorbed dose in lungs and m_{lung}[kg] gives the total mass of the lungs.

When radioisotope activity is converted to an absorbed dose, the effect of lung shunt must also be considered to avoid any overestimation of such results. Since the predicted absorbed dose includes only the applied activity localized in the liver as a whole [11], doses to the organs in close proximity of the liver cannot be calculated with this method bringing another source of uncertainty into calculations [9, 14].

To overcome or minimize the effect of these uncertainties on dosimetry calculations, we defined a procedure that included the MC approach to obtain organ doses in this study as an alternative to the dosimetry model of the mono-compartmental MIRD method. For MC simulations, we used a mathematical phantom tailored for each patient to incorporate the unique compositions and densities of certain structures such as liver, liver tumor, and lungs. As in the MIRD method, the lung shunt fraction (LSF) [11] of each patient was considered in the simulations based on which the Y-90 activity was fractionated between the patient's tumor and lung tissues, and the resulting activities within these volumes were homogeneously distributed. In addition, unlike MIRD studies in literature, the doses received by other organs such as the stomach wall, spleen, pancreas, and kidneys were also evaluated since these organs may be exposed to considerable radiation doses during the procedure because they reside close to the irradiated area.

This study aims to evaluate doses to tumor volume and neighboring organs during radioembolization patients and compare MIRD calculations based on clinical data and Monte Carlo simulations based on computer models. MCNP is a general-purpose MC code package that has found many uses, including radiation protection, shielding, dosimetry, medical physics, detector design and detector analysis, nuclear safety, waste management, decontamination, and service removal. In this study, version 6.1 of the code was employed which combines the capabilities of the MCNPX and MCNP5 codes [15, 16]. The simulations were performed on a desktop computer with Intel Core i5-5200U CPU @2.20 GHz, 16 GB RAM, and Linux Ubuntu 18.04 LTS.

In this study, a volumetric source with isotropic distribution was used which approximates the activity of ^{90}Y radioisotope source homogeneously distributed in the liver, tumor, and lung volumes of the patient, also considering the lung shunt fraction. For the energies of the beta particles to be emitted from the source, the source spectrum of ^{90}Y radioisotope was introduced into the code [17]. Since ^{90}Y is a beta emitter, only the electron option was chosen as the source particle type in MCNP.

In this study, the amount of energy released per particle in each volume of interest was recorded using tally (i.e., detector). Due to its maximum range of 11 mm and gamma penetration, ^{90}Y may reach to lungs, and other organs (stomach wall, pancreas, spleen, and kidneys) for liver tumors treatments. Thus, the gamma energies accumulated in these regions were also calculated.

Today, for patients treated using radioactive materials, calculation of doses in the tumor volume, in the adjacent critical organs, and in tissues before applying the therapy procedure, is an integral part of the treatment planning [16]. For this purpose, anthropomorphic models that imitate anatomical features of human body, called phantoms, have been created [18] and become useful tools. In this study, Oak Ridge National Laboratory (ORNL) phantom, a hermaphrodite phantom with both female and male characteristics adapted into MCNP, was used. The mass values of the source and critical organs in the ORNL phantom used in this study are given in table 3 [19].

The liver region of the phantom was divided into two: the right lobe (1224.5 cm^3) and the left lobe (605.5 cm^3), depending on the segmental anatomy of the liver within the scope of this study [20, 21]. In figure 1, cross-sectional MCNP images of the ORNL Hermaphrodite Phantom are shown.

Table 3. Masses of some organs (in kg) of the ORNL phantom [19].

Organs	Mass
Liver	1.903
Lungs	0.9975
Stomach wall	0.15808
Spleen	0.18304
Pancreas	0.09432
Kidneys	0.2995

[DOI: 10.61186/ijrr.21.3.353]

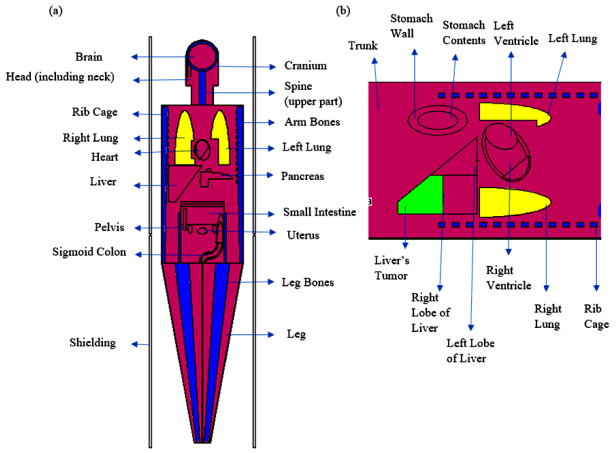

Figure 1. Cross-sectional images of the ORNL Hermaphrodite Phantom **(a)** coronal view and **(b)** axial view. The right and left lobes of the liver, the tumor area and adjacent structures of Patient 9 are given.

Statistical analysis

All statistical analyses were performed with IBM SPSS Statistics for Windows (Version 26.0 software) [22]. The Paired Samples *t-test* was applied to compare the means of dependent two-group data of the MIRD and MCNP dose results of the tumor and lung. The statistical difference was considered to be significant at $p<0.05$ values.

RESULTS

In this study, dosimetry calculations of 30 patients (22 men and 8 women) who went through radioembolization therapy were studied. The amount of ^{90}Y activity given to each patient was determined by the responsible physician. The mean injected ^{90}Y activity for the patients was 1.70 GBq (range: 0.67-2.90 GBq). For the Monte Carlo study of each patient, the liver of the ORNL phantom was divided into two parts: the tumor region and the surrounding liver tissue. Table 4 lists masses of these regions for each patient. As observed, healthy liver masses of the patients ranged from 0.0282 kg to 1.7134 kg while the tumor masses ranged from 0.1734 kg to 3.916 kg. Mean masses of liver and tumor volumes were calculated as 0.9916±0.4861 kg and 1.0196±0.7692 kg, respectively.

This study employs MCNP simulations to investigate the dosimetry uncertainties of MIRD methodology previously mentioned. The standard ORNL phantom was modified where liver volume of the phantom was reconstructed segmentally to incorporate the liver volume of each patient. In this manner, a separate input file was created for Monte Carlo simulations that yielded absorbed doses in liver, tumor and lung of each patient and the results were then compared with the calculations of MIRD method. In addition, the simulations determined absorbed doses in organs in proximity of liver such as stomach wall, spleen, pancreas, and kidneys for which MIRD calculation are not available. Considering the maximum penetration distance of beta particles emitted from Y-90 radioisotope, some damage to these organs is possible. Table 5 provides a summary of dose comparison between the MCNP simulations and MIRD calculations for the tumor tissue and lungs of each patient where the absorbed doses were normalized to corresponding source activity to express the results in units of Gy/GBq. The percentage differences of the doses calculated from MIRD method and simulated in MCNP for the tumor and lungs of the patients are given in figure 2.

Table 4. Mass (in kg) of healthy liver and tumor tissues.

Patient No	Healthy Liver	Tumor
1	1.3031	0.5473
2	0.8861	1.4343
3	0.9506	1.7918
4	1.1534	0.6524
5	1.7035	0.1734
6	0.9682	1.0160
7	0.6261	1.3324
8	0.9132	1.1926
9	1.2626	1.5375
10	1.3915	0.5077
11	1.7134	0.1700
12	0.2493	1.8644
13	0.4293	1.5923
14	1.4362	0.5255
15	0.3115	1.6286
16	0.4397	1.0815
17	1.3147	0.4781
18	1.1498	0.5439
19	0.9254	1.4054
20	1.2254	0.5791
21	0.0282	1.1717
22	0.4491	0.8869
23	0.1063	3.9160
24	0.5175	1.9327
25	1.0823	0.5308
26	1.4435	0.7109
27	1.4586	0.3553
28	1.4960	0.2905
29	1.2742	0.3776
30	1.5398	0.3623
Average	0.9916	1.0196
Standard Deviation	0.4861	0.7692

As seen in table 5, the lung shunt fractions of the patients ranged from 0 (Patients #17, #20, #27, and #29) to 0.17328 (Patient #24). These ratios were fractionated in the MCNP simulations equally between the right and the left lungs, and the ^{90}Y activity distribution was made accordingly. For the patients with no shunt, the lung doses were not calculated by the MIRD method and were thus considered not to be exposed to any dose. In addition, the MIRD calculations did not lead to any dose predictions in the organs around liver for which test

[DOI: 10.61186/ijrr.21.3.353]

Table 5. Treatment parameters and absorbed doses per unit activity for tumor and lungs calculated by MIRD and MCNP techniques.

Patient ID	Administered activity (GBq)	LSF	$D_{tumor, MIRD}$ (Gy/GBq)	$D_{tumor, MCNP}$ (Gy/GBq)	$D_{lung, MIRD}$ (Gy/GBq)	$D_{lung, MCNP}$ (Gy/GBq)
1	1.20	0.01568	89.92	84.80	0.784	0.710
2	1.55	0.02756	33.90	33.53	1.378	1.635
3	2.70	0.07061	25.93	25.88	3.531	3.212
4	0.67	0.02736	74.54	73.39	1.368	1.246
5	2.50	0.02736	280.46	270.59	1.368	1.254
6	1.80	0.01476	48.49	46.87	0.738	0.675
7	1.41	0.06931	34.93	34.84	3.465	3.131
8	1.41	0.05377	39.67	39.54	2.688	2.438
9	1.20	0.03339	31.43	30.02	1.670	1.513
10	1.90	0.05022	93.54	87.14	2.511	2.217
11	0.84	0.03938	282.53	236.83	1.969	1.780
12	2.90	0.01932	26.30	26.15	0.966	0.877
13	2.20	0.02709	30.55	30.50	1.355	1.235
14	2.00	0.02911	92.38	88.49	1.456	1.323
15	1.10	0.03841	29.52	29.28	1.920	1.742
16	2.04	0.02647	45.01	44.43	1.324	1.210
17	1.20	0.00000	104.58	101.13	-	0.001
18	0.80	0.05592	86.79	81.04	2.796	2.529
19	2.50	0.11273	31.57	31.62	5.636	5.070
20	2.07	0.00000	86.34	80.24	-	0.003
21	2.80	0.01739	41.93	41.09	0.869	0.796
22	1.00	0.05194	53.45	52.29	2.597	2.363
23	1.29	0.10804	11.39	11.55	5.402	4.865
24	2.71	0.17328	21.39	21.53	8.664	7.796
25	1.90	0.02222	92.10	89.30	1.111	1.006
26	2.40	0.02043	68.90	67.44	1.022	0.922
27	1.72	0.00000	140.73	129.49	-	0.003
28	0.77	0.04526	164.33	147.38	2.263	2.050
29	0.76	0.00000	132.42	115.90	-	0.007
30	1.55	0.02584	134.44	123.87	1.292	1.160
Average	1.70	0.04010	80.98	75.87	2.005	1.826
Standard Deviation	0.6813	0.03744	67.70	60.39	1.872	1.681
t			3.087		5.104	
p value			0.004		<0.001	

GBq, Gigabecquerel; LSF, Lung Shunt Fraction; Gy, Gray ; D, dose; MIRD, Medical Internal Radiation Dosimetry; MCNP, Monte Carlo N Particle.

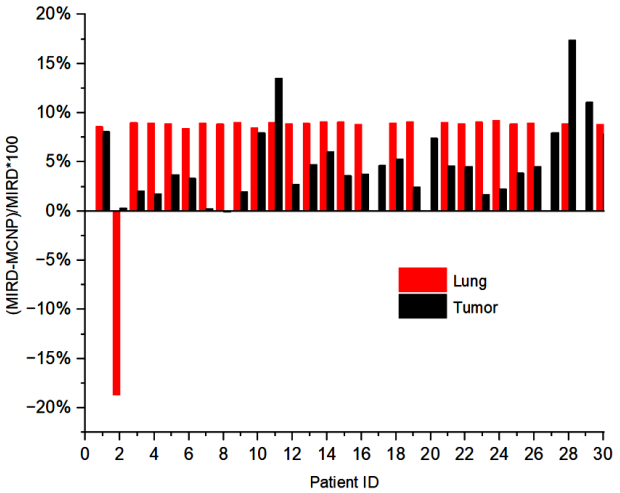

Figure 2. Percentage difference of doses from MIRD calculations and MCNP simulations for tumor and lungs of the patients.

angiography determined no activity distribution. However, MCNP simulations show that these organs were exposed to radiation doses and thus absorb some amount of dose, albeit relatively low.

The normalized dose results in table 5 for the tumor region ranged between a minimum of 11.39 Gy/GBq (Patient #23) and a maximum of 282.53 Gy/GBq (Patient #11) for MIRD with an average value of 80.98±67.70 Gy/GBq, the relatively high standard deviation of the results being due to the diversity of the liver and tumor masses as well as the administered activities which are determined based on the tumor size and the body tolerance of the patient. For example, the tumor mass of Patient 23, who was exposed to a relatively low radiation dose, is much larger than that of Patient 11, who was exposed to the highest radiation dose. On the other hand, Patient 11's activity is lower than that of Patient 23 which is not high enough to destroy such a tumor of large mass. Therefore, the dose of this patient's tumor area is lower than that for other patients. In addition, as seen in table 5, the results obtained with MCNP simulations for tumor tissue gave similar values compared to the results obtained with MIRD calculations. MCNP results ranged from a minimum of 11.55 Gy/GBq (Patient 23) to a maximum of 270.59 Gy/GBq (Patient 5), with a mean dose of 75.87±60.39 Gy/GBq. The tumor mass of Patient 23 is 3.916 kg and the activity value applied to this patient is 1.29 GBq, so the amount of activity per unit mass for this patient is less than that of Patient 5.

[DOI: 10.61186/ijrr.21.3.353]

Likewise, while the tumor mass of Patient 5 is 0.1734 kg, the applied activity is 2.5 GBq, and since the amount of activity per unit mass of this patient is higher than that of Patient 23, the dose of Patient 5 is higher. In the MIRD results, it was seen that Patient 11 received the highest tumor dose, while in the MCNP results, it was seen that Patient 5 received the highest tumor dose. The reason for this may be attributed to the geometry of the liver tumor defined in the MCNP simulations and its proximity to the lung.

As a goal of our study, the tumor and lung doses from both methods were mutually compared. It was observed that the difference between the MIRD and MCNP results for the tumor dose was at most 16.18%. As a result of this difference, one can safely state that MC simulations can be used both for dose verification and as an alternative to the MIRD method in the therapy of radioembolization patients.

The normalized dose results and the differences for the lung are also shown in table 5. The MIRD results for the lung tissue had a maximum of 8.664 Gy/GBq (Patient 24), a minimum of 0 Gy (Patients 17, 20, 27, and 29), and a mean of 2.005±1.872 Gy/GBq. The most important factor affecting the lung doses is the escape to the lung due to the activity given to the tumor area and the vascular structure of a patient. The lung escape ratio leads to an increase or decrease in the dose deposited into the lung. Two patients, namely Patient 19 (11.27% shunt ratio; male) and Patient 24 (17.32% shunt ratio; female), had maximum LSF values. When the lung dose results of these patients were evaluated, it was seen that these patients were exposed to the highest dose. Also, it is shown that lung doses from the MCNP simulations had a maximum of 7.796 Gy/GBq (Patient 24), a minimum of 0.001 Gy/GBq (Patient 17), and a mean of 1.826±1.681 Gy/GBq. The MCNP and MIRD results of patients 17, 20, 27, and 29 could not be compared because their shunt values were 0, and thus calculations could not be made with the MIRD method. While the lung doses received by these patients are accepted as 0 in the MIRD calculation, it is seen from the simulations that the lungs of these patients are exposed to some amount of radiation dose even though they do not contain any activity due to leakage. In table 5, the normalized MIRD and MCNP results of Patients 19 and 24 with high shunt ratios were found to be higher than other patients. According to these results, it was observed that both MIRD and MCNP dose results increased in direct proportion with the lung shunt ratio. When the dose results of MC simulations for the lung and MIRD dose results were compared, the difference was observed to be a maximum of 11.69%. As a result of this difference value, it was predicted that MC simulations could be used as an alternative for therapy planning in the radioembolization method. In addition, since the upper limit of the lung dose absorbed for the ^{90}Y glass microspheres used in this study was accepted to be in the range of 25 and 30 Gy in a single therapy and 50 Gy in the cumulative therapy, it was observed that the results obtained here were below these values.

It should be noted that the MIRD and MCNP methods used in our dose calculation study represent fundamentally different situations. While the former makes a general dose calculation based on equations, the latter treat the transport of radiation in tissue environment probabilistically. In addition, all possible interaction mechanisms of beta particles in the environment were evaluated in our simulations and the results were obtained as such.

DISCUSSION

Our results compare well with those reported by other research groups. The study by Petitguillaume et *al.* used patient-specific data and Monte Carlo simulations performed in 2013 for three-dimensional personal dosimetry of ten patients treated with resin microspheres [23]. Clinical data (internal dosimetry method/partition model) and simulation results were compared. MCNPX input files were created using OEDIPE software and a voxelized phantom was employed. Using equation (1), the difference between Partition model and Monte Carlo simulation results was found to be 27%. In our study, the difference between the MIRD and MCNP results was lower than 11.69% for lung and 16.18% for tumor. The reason for this difference may be the larger number of patients participating in our study, the variability of the applied activity among the patients, and the placement of tumors in different geometries by the liver tumor region of each patient by segmenting the liver of the MIRD phantom.

In a similar study by Hashikin et *al*. in 2017, Geant4 Monte Carlo simulations and the partition model calculation were used on 28 patients [24]. A mathematical adult human phantom model created according to MIRD Pamphlet 5 was defined in Geant4 and a single tumor was placed in the center of the mathematical liver phantom. The Models containing two tumors of the same size, two tumors of different sizes, and four tumors of the same size were created, and the simulations were performed accordingly. ^{90}Y spheroids each with 300 Bq activity were homogeneously distributed in the liver. Using equation (1), the difference between clinical and simulation data was found to be 11.74% for lungs and 8% for tumors. In our study, the MCNP simulations and the MIRD method were used on 30 patients where the difference between the MIRD and MCNP results was below 11.69% for lung and 16.18% for tumor. The main reason for this difference is that the geometry and volume of the tumor are specific to each patient and the applied

[DOI: 10.61186/ijrr.21.3.353]

activity is higher than the study by Hashikin *et al.* [24]. In our study, the liver of the MIRD phantom was segmented and tumors of different geometries were placed by the liver tumor region of each patient, and although the applied activity was different for each patient, it was homogeneously distributed at an average value of 1.70 GBq. The differences between our study and other studies can be seen in table 6.

Table 6. Comparison of the results from our study with those from similar studies in the literature.

Quantities	This Study	Petitguillaume *et al.* 2013 [23]	Hashikin *et al.* 2017 [24]
Internal Dosimetry Method	MIRD Model	Partition Model	Partition Model
Monte Carlo Simulation Code	MCNP	MCNPX	GEANT4
Phantom Type	MIRD Phantom	Voxelized Phantom	MIRD Model
Number of Patients	30	10	28
Activity (GBq)	1.70 (average)	-	3.10^{-7}
Microsphere Type	Glass microsphere	Resin microsphere	-
MC and MIRD % Difference for Tumor	16.18	27	8
MC and MIRD % Difference for Lung	11.69	-	11.74

Since the MIRD method assumes a uniform material density and composition for each organ or tissue, remarkable differences between human tissues are usually neglected [13]. In addition, lung doses can be calculated by considering only the liver, tumor, and shunt ratio with the MIRD equation, and the contributions of radiation penetrating to other organs are neglected beyond a certain distance. This may lead to inaccuracies or uncertainties in dose calculations. In our study, considering the maximum penetration of the ^{90}Y radioisotope, the doses taken by the organs close to the liver were also evaluated as given in table 7.

As a result of the MCNP simulations, it has been shown that organs such as stomach wall, spleen, pancreas, and kidneys, whose doses cannot be calculated in the MIRD method, are exposed to a certain amount of dose. Stomach wall results were observed to be maximum for Patient 1 for which the organ in question resides closer to the left lobe of the liver and the tumor is in the left lobe of the liver. As can be seen in table 4, the tumor area for this patient covers almost the entire left lobe. It is usual for this patient to be exposed to the maximum dose due to the applied activity and because the stomach wall is close to the left lobe. The spleen is located behind the stomach, close to the right lobe of the liver. In table 7, it is shown that the maximum dose for the spleen belongs to Patient 10. This patient's tumor was inside the right lobe and a relatively higher activity of 1.90 GBq was applied. Due to the tumor location of the patient and the applied activity, this patient received the maximum dose for the spleen. Another organ close to the right lobe of the liver is the pancreas, and Patient 2 received the maximum dose for this organ, whose right lobe study was performed and whose mass included most of the right lobe, as can be seen in table 4. This patient received 1.55 GBq of Y-90 activity, and because of this activity and the size of the tumor volume, the pancreas was also exposed to a certain dose during this patient's therapy. The last critical organ to be evaluated in our study is the kidneys which are usually located near the exit of the right lobe towards the lower part of the liver. Since the tumor location of Patient 3 was in both the right lobe and the left lobe and high activity of 2.70 GBq was applied to this patient, the kidneys were exposed to the maximum dose in the therapy of this patient. The minimum dose in all these critical organs, whose dose results were calculated by means of the simulation, was taken in the therapy of Patient 28. This is because the patient's tumor site is in a small area in the deep part of the right lobe and low activity of 0.77 GBq was applied.

Table 7. Normalized doses (in mGy/GBq) calculated by MCNP received by organs close to the liver.

Patient No	Stomach wall	Spleen	Pancreas	Kidneys
1	5.632	1.846	13.377	1.660
2	0.857	0.584	23.355	3.683
3	1.814	1.301	5.766	33.612
4	1.251	0.665	3.116	4.300
5	1.549	0.633	3.323	2.564
6	0.488	0.470	2.258	6.084
7	1.018	0.799	2.897	3.489
8	0.697	0.502	2.486	2.939
9	0.849	0.506	3.545	3.786
10	1.797	4.093	3.170	1.274
11	2.213	0.794	5.470	1.582
12	1.267	0.823	4.932	3.221
13	1.200	0.836	4.563	3.478
14	1.929	1.582	8.683	3.115
15	1.400	0.924	4.193	2.275
16	1.123	0.577	3.704	3.777
17	1.052	0.616	2.522	3.509
18	1.220	0.590	2.442	5.161
19	0.829	0.687	3.116	3.388
20	5.103	1.743	11.813	1.930
21	1.145	0.606	4.843	3.615
22	1.196	0.595	4.128	3.529
23	0.827	0.805	2.470	2.438
24	1.144	0.918	2.896	2.780
25	1.260	0.827	3.967	3.976
26	0.006	0.003	0.009	0.004
27	4.634	1.985	12.072	1.879
28	0.003	0.001	0.003	0.014
29	0.452	0.270	1.835	1.481
30	0.180	0.343	1.057	2.191
Average	1.488	0.897	4.934	3.891
Standard Deviation	3.545	0.770	4.751	5.767

CONCLUSION

In this study, tumor volumes of 30 patients were determined based on their CT images, and a mathematical phantom was also modified to include patient-specific liver regions to be used in Monte Carlo simulations for organ dose calculations from ^{90}Y administration. It has been observed that the simulations yield more precise results in a shorter time interval, along with the possibility of allowing all organs to be considered for a more precise dose

[DOI: 10.61186/ijrr.21.3.353]

planning. Therefore, according to our findings, Monte Carlo simulations can be used in the clinic for dose verification of the MIRD method and, in addition, as an alternative to the MIRD method.

ACKNOWLEDGMENT

The authors do not have any commercial or other association that might pose a conflict of interest.

***Ethical Considerations*:** All subjects gave their informed consent for inclusion before they participated in the study. The study was conducted in accordance with the Declaration of Helsinki, and the protocol was approved by the Ethics Committee of Koc University (Istanbul, Turkey) Faculty of Medicine Clinical Research (Date: 30.10.2019/ No: 2019. 098.IRB1.010).

***Funding*:** Self-funding.

***Conflicts of interests*:** The authors declare no conflict of interest.

***Author contributions*:** Conceptualization, O.Y., A.B.*, A.B and M.O.; methodology, O.Y., A.B.*, A.B. and M.O.; writing-original draft preparation, O.Y.; writing-review and editing, A.B.*, A.B. and C.C.; supervision, A.B.* All authors have read and agreed to the published version of the manuscript.

REFERENCES

1. Kim SP, Cohalan C, Kopek N, Enger SA (2019) A guide to ^{90}Y radioembolization and its dosimetry. *Phys Medica, **68**: 132-145.*
2. Braat AJAT, Smits MLJ, Braat MNGJA, Manon NGJA, et al. (2015) ^{90}Y Hepatic radioembolization: an update on current practice and recent developments. *J Nucl Med*, ***56**(7): 1079-87.*
3. Dezarn WA, Cessna JT, Dewerd LA, Feng W, *et al.* (2011) Recommendations of the American Association of Physicists in Medicine on dosimetry, imaging, and quality assurance procedures for 90Y microsphere brachytherapy in the treatment of hepatic malignancies. *AAPM, **38**(8): 4824-45.*
4. Cross WG, Böhm J, Charles M, Piesch E, Seltzer SM (2016) Report 56: Dosimetry of external beta rays for radiation protection. *J ICRU, **29**(1): 1473-6691*.
5. Salem R and Thurston KG (2006) Radioembolization with 90Yttrium microspheres: a state-of-the-art brachytherapy treatment for primary and secondary liver malignancies. Part 1: Technical and methodologic considerations. *J Vasc Interv Radiol*, ***17**(8): 1251-78.*
6. Mitchell GS, Lloyd PNT, Cherry SR (2020) Cerenkov luminescence and PET imaging of (90)Y: capabilities and limitations in small animal applications*. Phys Med Biol, **65**(6): 65006-065006.*
7. Jackson JD. Classical electrodynamics. American Association of Physics Teachers; 1999.
8. Krane KS. Introductory nuclear physics. John Wiley & Sons; 1991.
9. Danieli R, Milano A, Gallo S, Veronese I, Lascialfari A, *et al.* (2022) Personalized dosimetry in targeted radiation therapy: A look to methods, tools and critical aspects*. J Pers Med, **12**(2): 205.*
10. Auditore L, Amato E, Italiano A, Arce P, *et al.* (2019) Internal dosimetry for TARE therapies by means of GAMOS Monte Carlo simulations. *Phys Med Biol, **64**: 245-251.*
11. Villalobos A, Soliman MM, Majdalany BS, Schuster DM, *et al.* (2020) Yttrium-90 radioembolization dosimetry: what trainees need to know. *Semin Interv Radiol*, ***37**(5): 543-554.*
12. Graves SA and Hobbs RF (2021) Dosimetry for optimized, personalized radiopharmaceutical therapy. *Semin Radiat Oncol, **31:** 37-44*.
13. Cremonesi M, Chiesa C, Strigari L, Ferrari M, *et al.* (2014) Radioembolization of hepatic lesions from a radiobiology and dosimetric perspective. *Front Oncol, **4**: 210.*
14. Giammarile F, Bodei L, Chiesa C, Flux G, *et al.* (2011) EANM procedure guideline for the treatment of liver cancer and liver metastases with intra-arterial radioactive compounds. *EANMI, **38** (7): 1393-406.*
15. Goorley T, James M, Booth T, Brown F, *et al.* (2012) Initial MCNP6 Release Overview. *Nucl Technol, **180**(3): 298-315.*
16. Reed AL (2007) Medical physics calculations with MCNP: a primer. ANS Meeting, 836.
17. Jodal L (2009) Beta emitters and radiation protection. *Acta Oncol, **48**(2): 308-13*
18. Zankl M, Becker J, Schlattl H, Henss N, *et al.* (2007) Computational Phantoms of the ICRP Reference Male and Reference Female. *Radiat Prot Dosim, **127**(1-4): 174-86.*
19. Synder WS, Cook MJ, Nasset ES, Karhausen LR, *et al.* (1974) Report on the task group on Reference Man; Pergamon Press, Oxford.
20. Abdalla EK, Denys A, Chevalier P, Nemr RA, Vauthey JN (2004) Total and segmental liver volume variations: implications for liver surgery. *Surgery,**135**(4): 404-10.*
21. Wolf DC (1990) Evaluation of the size, shape, and consistency of the liver. Clinical Methods: The History, Physical, and Laboratory Examinations. 3rd ed. Boston: Butterworths; 1990.
22. IBM SPSS Statistics for Windows V. IBM Corp. Released Armonk, NY: IBM Corp; 2019.
23. Petitguillaume A, Bernardini M, Hadid L (2014) Three-dimensional personalized Monte Carlo dosimetry in Y-90 resin microspheres therapy of hepatic metasases: nontumoral liver and lungs radiation protection considerations and treatment planning optimization. *J Nucl Med, **55** :405-413.*
24. Hashikin NAA, Yeong CH, Guatelli S, Abdullah BJJ, *et al.* (2017) Systematic investigation on the validity of partition model dosimetry for (90)Y radioembolization using Monte Carlo simulation. *Phys Med Biol, **62**(18): 7342-7356.*

[DOI: 10.61186/ijrr.21.3.353]